

---

# 360VFI: A Dataset and Benchmark for Omnidirectional Video Frame Interpolation

**Wenxuan Lu**  
*School of Computer Science  
Wuhan University*

*wenxuanlu@whu.edu.cn*

**Mengshun Hu**  
*School of Computer Science  
Wuhan University*

*shunmh@whu.edu.cn*

**Yansheng Qiu**  
*School of Computer Science  
Wuhan University*

*qiuyansheng@whu.edu.cn*

**Liang Liao**  
*School of Computer Science  
Wuhan University*

*liang.liao@ntu.edu.sg*

**Zheng Wang**  
*School of Computer Science  
Wuhan University*

*wangzwhu@whu.edu.cn*

## Abstract

With the development of VR-related techniques, viewers can enjoy a realistic and immersive experience through a head-mounted display, while omnidirectional video with a low frame rate can lead to user dizziness. However, the prevailing plane frame interpolation methodologies are unsuitable for Omnidirectional Video Interpolation, chiefly due to the lack of models tailored to such videos with strong distortion, compounded by the scarcity of valuable datasets for Omnidirectional Video Frame Interpolation. In this paper, we introduce the benchmark dataset, 360VFI, for Omnidirectional Video Frame Interpolation. We present a practical implementation that introduces a distortion prior from omnidirectional video into the network to modulate distortions. We especially propose a pyramid distortion-sensitive feature extractor that uses the unique characteristics of equirectangular projection (ERP) format as prior information. Moreover, we devise a decoder that uses an affine transformation to facilitate the synthesis of intermediate frames further. 360VFI is the first dataset and benchmark that explores the challenge of Omnidirectional Video Frame Interpolation. Through our benchmark analysis, we presented four different distortion conditions scenes in the proposed 360VFI dataset to evaluate the challenge triggered by distortion during interpolation. Besides, experimental results demonstrate that Omnidirectional Video Interpolation can be effectively improved by modeling for omnidirectional distortion.

# 1 Introduction

In pursuit of a realistic visual experience, omnidirectional videos (ODVs), also known as 360° videos or panoramic videos, have obtained research interest in the computer vision community and become an essential basis of augmented reality (AR) and virtual reality (VR). To have a continuous and immersive experience, ODVs require an extremely high frame rate. However, because of the high industrial cost of high-precision camera sensors, the frame rates of most ODVs are relatively low.

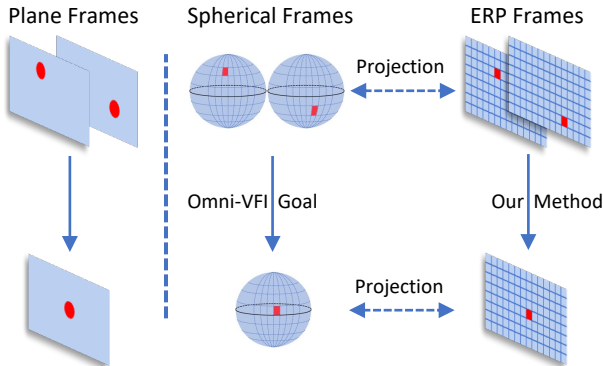


Figure 1: Left: Traditional Video Frame Interpolation: The inputs are two adjacent plane frames and the output is a target plane frame. Right: Omnidirectional Video Frame Interpolation: The inputs are two adjacent omnidirectional frames with a full field-of-view from an omnidirectional video and the output is a target omnidirectional frame. Original-formatted omnidirectional frames are spherical and the most common format is Equirectangular projection (ERP). The two kinds of omnidirectional video formats can be projected from each other and our proposed method tackled ERP videos.

Traditional Plane Video Frame Interpolation (Plane VFI) techniques have emerged as a basic solution to address the challenges of low frame rates. The development of optical flow networks (Dosovitskiy et al., 2015; Sun et al., 2018; Teed & Deng, 2020; Kong et al., 2021) has led to notable progress in flow-based Plane VFI methods (Jiang et al., 2018a; Xu et al., 2019; Niklaus & Liu, 2020; Park et al., 2021). This is attributed to the capability of optical flow to establish explicit correspondences for frame registration in video frame sequences. Flow-based methods typically follow a three-step process: First, estimate the optical flow between two input frames and an arbitrary target frame. Then warp the input frames or context features using predicted flow fields for spatial alignment. Finally, refine warped frames or features and generate the target frame using a synthesis network. Recently, IFRNet (Kong et al., 2022) was proposed to benefit intermediate flow and intermediate feature with each other, with the ability to generate sharper moving objects and capture better texture details. Similarly, in the omnidirectional domain, interpolating frames via optical flow is effective but not efficient. Omnidirectional optical flow estimation has been explored recently. In SLOF (Bhandari et al., 2022), ERP video frames were re-projected onto the sphere to apply rotational augmentation. In MPF (Li et al., 2022), the ERP format frames were transformed into multiple types of projection formats, and these different projection formats were fused to learn a more precise flow. However, these two works have not considered using ERP distortion as prior knowledge. Therefore, it is not efficient to use their estimated optical flow to interpolate omnidirectional frames. As shown in Figure 1, ODVs are typically stored and transmitted in equirectangular projection (ERP) format, which introduces distortions. So traditional frame interpolation methods struggle to handle effectively. Consequently, dealing with ERP video frames directly using distortion as prior knowledge is an effective and efficient way.

Datasets for plane VFI tasks have been sufficiently researched, including Vimeo90K (Xue et al., 2019), UCF101 (Soomro et al., 2012), and SNU-FILM (Choi et al., 2020). Vimeo90K is the most popular dataset for plane VFI, which is composed of triplet samples. However, Vimeo90K is not designed for motion extent, and this is very important in Omnidirectional Video Interpolation because of its latitude-dependent distortion. SNU-FILM was proposed for the motion-based interpolation benchmark. Both are focused on Plane VFI. Recently, omnidirectional video datasets have caught the attention of the computer community. A few

---

datasets were proposed for Omnidirectional Video Super-Resolution including ODV360 (Wang et al., 2023), 360VDS, and 360UHD (Baniya et al., 2023). They are collected from both Youtube and by themselves. Therefore, there are no Omnidirectional Video Frame Interpolation (Omni-VFI) datasets that have both sufficient and various samples.

To alleviate these problems, we introduce a dataset for Omnidirectional Video Interpolation, called 360VFI dataset. Besides, we also propose a benchmark (360VFI), which injects the omnidirectional distortion into the network, based on the 360VFI dataset. Specifically, in the 360VFI dataset, our evaluation benchmark has four different settings. We classified the triplets based on vertical motion extent due to the latitude-dependent distortion in the omnidirectional frame. In 360VFI Network, we propose the DistortionGuard module to extract less distorted pyramid features from input frames. Moreover, we propose OmniFTB to gradually refine a distorted ERP target frame. Experimental results demonstrate that the Omnidirectional Video Interpolation can be effectively improved by modeling for omnidirectional distortion.

Overall, this paper makes the following contributions:

- We present the first Omnidirectional Video Frame Interpolation (Omni-VFI) datasets 360VFI covering of various motion and content.
- We propose a benchmark for evaluating Omni-VFI in different vertical motion, and our 360VFI Net successfully improves Omni-VFI performance.
- Our experiments demonstrate that 360VFI achieves SOTA performance on the proposed benchmarks by considering omnidirectional priors in both feature extraction and frame generation, especially in the scene of large motion omnidirectional frame interpolation.

## 2 Related Work

### 2.1 Omnidirectional Data Processing

Omnidirectional images and videos have been attracting increasing attention from computer vision and graphics researchers. Due to the special representation of omnidirectional images, dedicated methods were developed for analysis and processing tasks, such as depth estimation (Wang et al., 2020a), salient object detection (Li et al., 2019b; Wu et al., 2022; Monroy et al., 2018; Zhang et al., 2018), edit propagation (Zhang et al., 2021), and video stabilization (Kopf, 2016; Tang et al., 2019). With the recent development of immersive technologies, researchers have been working on the specific problems of omnidirectional video-based applications, such as automatic 360° navigation (Kang & Cho, 2019; Hu et al., 2017), omnidirectional video assessment (Li et al., 2019a), and immersive video editing (Nguyen et al., 2017). However, the absence of consistent temporal correspondences poses challenges for various applications, including Omni-VFI. In response to this challenge, our method aims to address the lack of reliable temporal correspondences in omnidirectional video processing. Furthermore, significant research (Esteves et al., 2018; Cohen et al., 2018) has focused on omnidirectional or 360° data, including spherical and ERP data, aimed at learning sphere representations

Most convolutional networks were initially designed to project images onto flat surfaces like traditional camera sensors. To extend their applicability to spherical images, researchers have proposed various solutions aimed at enabling convolutions on such images to facilitate feature extraction and interpretation by deep networks. A notable method, known as SphereNet (Coors et al., 2018; Yang et al., 2021), adjusts the perceptual field of its convolutional kernels based on the latitude within the ERP domain. However, altering the kernels of 2D optical flow networks to spherical kernels may compromise the effectiveness of pre-trained models. To address this issue, the kernel transform technique (Su & Grauman, 2019) has been explored, allowing convolutional layers to learn how to transform spherical kernels to the pre-trained weights of standard kernels initially trained on perspective images. Nevertheless, the significant number of layers in current optical flow networks poses practical challenges in terms of computation and memory costs associated with learning to transform all layers. Therefore, further research and improvements are necessary to overcome these obstacles and enhance their applicability in the domain of omnidirectional image and video processing.

---

## 2.2 Video Frame Interpolation

Video Frame Interpolation aims at generating non-existent frames between two adjacent input frames. In Long et al. (2016), a pioneering learning-based method was proposed that can directly synthesize intermediate frames between two frames. Consequently, frame interpolation methods based on spatially adaptive convolution kernels (Niklaus et al., 2017; Lee et al., 2020; Cheng & Chen, 2021) or pixel phases (Meyer et al., 2015; 2018) were proposed. However, the former leads to large parameters and high complexity, especially when dealing with complex motion. The latter has difficulty handling complex motion due to an inaccurate estimation of phase and amplitude values. After that, many flow-based methods (Jiang et al., 2018b; Xue et al., 2019) use optical flow to guide warping, but the inaccuracy of the predicted optical flow usually causes distortion of the result, so extra measures (Bao et al., 2019; 2018) are usually taken to refine the warped frame. Some methods generate intermediate frames directly like CAIN (Choi et al., 2020) using channel attention and RIFE (Huang et al., 2022) using distillation to get a good result from one simple architecture. IFRNet (Kong et al., 2022) proposes a novel single encoder-decoder-based method to jointly perform intermediate flow estimation and intermediate feature refinement for efficient VFI, which also performs real-time inference with excellent accuracy. All Video Frame Interpolation methods mentioned above cannot generate well on omnidirectional frames because they are not designed for them. Additionally, to our best knowledge, few methods have been proposed for Omni-VFI.

## 2.3 Conditional Modeling and Integration

Many real-world problems require the integration of multiple sources of information. When dealing with such issues, it often makes sense to process one source of information within the context provided by other prior knowledge. In the realm of machine learning, this contextual processing is often termed conditioning: the computations performed by a model are influenced or adjusted by prior knowledge derived from an auxiliary input. In Dumoulin et al. (2018), feature-wise transformations within many neural network architectures prove to be highly efficient in addressing a remarkably vast and diverse array of problems. Their success can be attributed to their adaptability in acquiring an effective representation of the conditioning input across various scenarios.

In OSRT (Yu et al., 2023), a distortion-aware transformer used for omnidirectional image super-resolution was proposed. They take the ERP distortion priors as a condition in the attention mechanism to modulate distortion. Specifically, OSRT deforms the feature maps using offsets calculated from the latitude-dependent conditions, continuously and adaptively modulating and encoding the ERP distortion into the network, achieving modeling and correction of the ERP distortion. The Spatial Feature Transform (SFT) (Wang et al., 2018) uses semantic segmentation probability maps as categorical priors to provide useful conditioning information for the image super-resolution task. Specifically, the low-resolution input image is first passed through a semantic segmentation network to obtain the corresponding probability maps, which represent the probability of each pixel belonging to different semantic classes (e.g., sky, building, vegetation, etc.). Then, a novel Spatial Feature Transform (SFT) layer takes these probability maps as conditions, learns to generate scaling parameters specific to each semantic class, and uses them to modulate the intermediate feature maps. This allows the generated high-resolution image to have more realistic and intricate textural details consistent with the corresponding categories.

## 2.4 Omnidirectional Datasets

While datasets for plane VFI tasks have been extensively researched, including Vimeo90K (Xue et al., 2019), UCF101 (Soomro et al., 2012), and SNU-FILM (Choi et al., 2020), there is a lack of dedicated datasets for Omni-VFI. Leveraging existing datasets can streamline the benchmark creation process for Omni-VFI, ensuring standardization and reducing the learning curve for researchers. However, there is no dataset used in the computer vision community directly for Omni-VFI. Thanks to the contributions of Wang et al. (2023) and S3PO (Baniya et al., 2023), high-resolution ODV super-resolution datasets ODV360, 360VDS, and 360UHD have been introduced, which can be utilized in Omni-VFI.

### 3 360VFI Dataset

To advance the development of Omni-VFI, a comprehensive dataset is paramount. We present a novel dataset curated from multiple sources and tailored specifically for Omni-VFI. Our dataset amalgamates three distinct collections, denoted as ODV360, 360VDS, and 360UHD, each contributing unique insights and challenges to the Omnidirectional Image Super-Resolution domain. We removed all dirty and unsuitable data and recollected it for the frame interpolation task.

#### 3.1 ODV360, 360VDS and 360UHD

ODV360 (Wang et al., 2023) is a novel high-resolution (4K-8K) ODV dataset curated to address the scarcity of high-quality video datasets in the field of omnidirectional video super-resolution. It comprises 90 videos sourced from YouTube and public omnidirectional video repositories, alongside an additional 160 videos captured using Insta360 cameras, including models such as Insta 360 X2 and Insta 360 ONE RS. The dataset covers a diverse range of content spanning indoor and outdoor scenarios, downsampled to a standardized 2K resolution (2160x1080) for ease of use in ODV super-resolution.

360VDS and 360UHD are both proposed in S3PO (Baniya et al., 2023). They created a new dataset of Omnidirectional Videos specifically designed for super-resolution termed 360VDS. Open-source datasets used in other areas of 360° video research were assembled to create the 360VDS. Additionally, they also made use of the publicly available 360° video dataset from the Stanford VR lab called psych-360 (Miller et al., 2020). They also created a 360 Ultra High-Definition (360UHD) dataset, consisting of eight clips ranging from HD to 4K.

#### 3.2 Proposed 360VFI Dataset

Table 1: Comparisons Between Different Video datasets.

	Modality	Task	Partition	Scenarios			
				Indoor	Outdoor	People	Landscape
Vimeo90K (Xue et al., 2019)	Plane Video	VFI	×	✓	✓	✓	×
CAIN (Choi et al., 2020)	Plane Video	VFI	✓	✓	✓	✓	×
ODV360 (Wang et al., 2023)	360° Video	360° VSR	×	✓	✓	✓	✓
360VDS (Baniya et al., 2023)	360° Video	360° VSR	×	×	✓	✓	✓
360UHD (Baniya et al., 2023)	360° Video	360° VSR	×	×	✓	✓	✓
SUN360 (Torralba, 2012)	360° Image	360° OLSE	×	✓	✓	✓	✓
360-SOD (Zhao et al., 2023)	360° Image	360° OD	×	×	✓	×	×
<b>360VFI(Ours)</b>	360° Video	360° VFI	✓	✓	✓	✓	✓

Table 2: Motion (latitude flow magnitude) statistics for each setting in 360VFI.

	Easy	Middle	Hard	Extreme	All
Triplets	518	260	76	76	930
Extent	[0, 2]	[2, 3]	[3, 4]	[4, 10]	[0, 10]

Our 360VFI dataset adopts a similar format as Vimeo90K (Xue et al., 2019). Each sample in our dataset consists of a triplet of video frames. Notably, the first and third frames are designated as input frames for the Omni-VFI model, while the second serves as the ground truth target frame. In the ODV360 (Wang et al., 2023) dataset, each video comprises 100 frames, while in the 360VDS and 360UHD (Baniya et al., 2023) dataset, the videos consist of 20 frames. We omit the final frame from each video in the ODV360 dataset, resulting in 99 frames per video, which are subsequently divided into 33 triplets. For videos in the 360VDS and 360UHD datasets, the first and last frames are discarded, leaving 18 frames per video, which

are divided into 6 triplets. Each triplet constitutes an independent sample and the whole dataset consists of 930 triplets. This comprehensive arrangement enables a holistic evaluation of interpolation algorithms against genuine ODV content. We randomly divide these videos into training and testing sets.



Figure 2: Examples of Different Scenarios in 360VFI Dataset

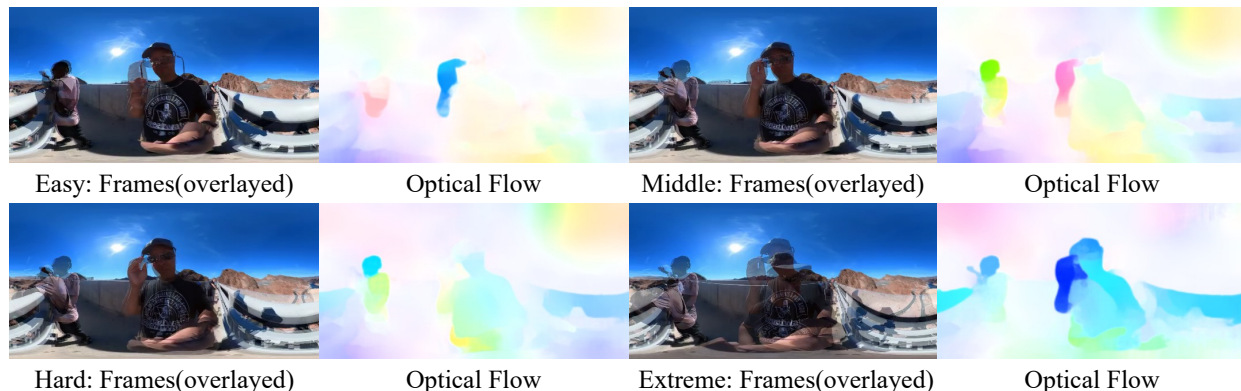


Figure 3: Input Frames and Optical Flow of Different Settings in 360VFI Dataset. The colored parts in the optical flow image are larger and deeper when the motion is larger. The motion increases from the easy setting to the extreme setting.

Videos in our dataset cover various scenarios, including natural landscapes, playgrounds, interiors of houses and cars, and indoor markets, as shown in Figure 2. To facilitate nuanced evaluations and benchmarking, we stratified the dataset into four distinct settings based on the varying degrees of motion inherent within the omnidirectional scenes, ranging from 0.19 to 9.69. These settings are categorized as easy, middle, hard, and extreme; the triplet numbers and their respective storage are illustrated in Table 2. The motion ranges for these settings are as follows:  $[0.19, 2]$ ,  $[2, 3]$ ,  $[3, 4]$ , and  $[4, 9.69]$ . The frames and optical flow of different partitions are illustrated in Figure 3. This stratification allows researchers to systematically assess the performance of their models across varying levels of motion complexity, facilitating a deeper understanding of model robustness and generalization capabilities. In Table 1<sup>1</sup>, we compare the 360VFI dataset with other datasets. These datasets include plane video, 360° video, and 360° images. Our dataset is the first one composed of 360° video for Omnidirectional Video Interpolation. Our dataset establishes a solid foundation for future research in Omni-VFI. By amalgamating diverse datasets and incorporating motion-based stratification, it not only enriches the existing repository of ODV data, but also sets a precedent for structured evaluation and benchmarking in this evolving field. We anticipate that our dataset will serve as a catalyst for innovation and foster the development of more sophisticated and resilient Omnidirectional Video Interpolation models in the future.

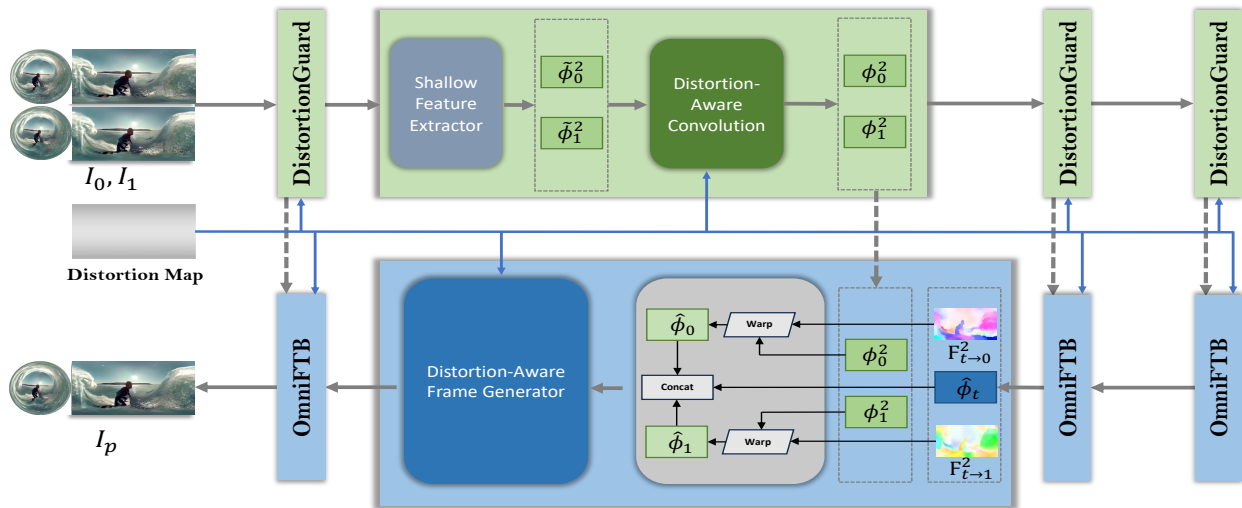


Figure 4: Architectural Overview. Our model is an efficient encoder-decoder based network, which first extracts less distorted pyramid context features  $\phi_0^l$  and  $\phi_1^l$  from input omnidirectional frames  $I_1, I_2$  with DistortionGuards, and then gradually refines bilateral intermediate flow fields  $F_{t \rightarrow 0}^l$  through OmniFTB generator, until yielding the target frame  $I_p$ . The figure above gives an illustration of the second-level DistortionGuard and OmniFTB, and details are shown below in Figure 6 and Figure 7.

## 4 Method

Given two adjacent omnidirectional video frames  $I_1$  and  $I_2$ , Omni-VFI aims at generating a non-existent intermediate omnidirectional frame  $I_p$  to enhance visual quality and consistency between adjacent frames, which is as similar as possible to ground truth frame  $I_g$ . Current plane VFI methods use networks to directly learn a mapping function  $G_\theta$  parametrized by  $\theta$  as

$$I_p = G_\theta(I_1, I_2). \quad (1)$$

In order to generate  $I_p$ , a specific loss function  $\mathcal{L}$  is designed for Omni-VFi to optimize  $G_\theta$  on the training samples,

$$\hat{\theta} = \operatorname{argmin}_{\theta} \sum_i \mathcal{L}(I_p, I_g), \quad (2)$$

where  $(I_1, I_2, I_g)$  are training pairs.

We show that ERP distortion prior, i.e., knowing that the distortion in omnidirectional frames is latitude-dependent, is beneficial to generate a more accurate intermediate frame. The prior knowledge  $\Psi$  can be conveniently represented by the ERP distortion condition map  $C_d$  and we will explore more details about  $C_d$  in Section 4.1,

$$\Psi = C_d. \quad (3)$$

To introduce priors in Omni-VFI, we reformulate equation 1 as

$$I_p = G_\theta(I_1, I_2 | \Psi), \quad (4)$$

where  $\Psi$  defines the prior upon which the mapping function can condition. As mentioned in Section 2.3, there are many work using prior knowledge to guide their task in other computer vision tasks. Hence, we propose 360VFI Net, including DistortionGuard and OmniFTB.

<sup>1</sup>VFI: Video Frame Interpolation; VSR: Video Super-Resolution; OLSE: Outdoor Light Source Estimation; OD: Object Detection

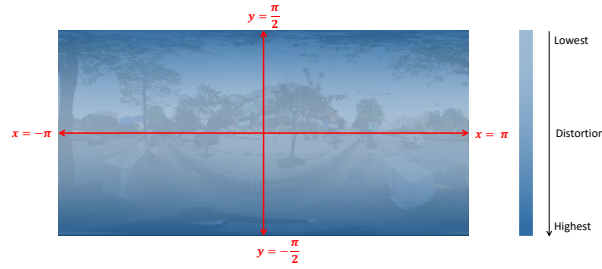


Figure 5: Illustration of an ERP frame and the distortion condition. The extent of distortion is the most severe in the polar regions.

#### 4.1 Distortions in Omnidirectional Video

ERP is a projection method used to map spherical surfaces onto a plane. In ERP, every point on the sphere is mapped onto the plane in such a way that each line from the polar center point maintains the same distance. So the distortion of ERP is latitude-dependent and all the pixels at the same height have the same distortion extent. This projection is frequently utilized in the creation of omnidirectional images and videos to depict environments more authentically and naturally, as it maintains depth and distance perception while minimizing distortion. As ODIs under different projection types are constrained by different transforming equations, the distortion caused by each type is inconsistent. ERP is the most convenient projection type for storage or transmission. To explain the causation of distortions more effectively, we follow the definition of stretching ratio ( $\mathbf{K}$ ) in Sun et al. (2017a), which signifies the degree of distortion at various locations, measured from the desired projection type to the ideal spherical surface.  $\mathbf{K}$  is determined by the variation in the area from one type of projection to another. As shown in Figure 5, the coordinate in ERP is defined as  $x$  and  $y$ . ERP stretching ratio can be derived as

$$\mathbf{K}_{\text{ERP}}(x, y) = \frac{\delta S}{\delta P} = \cos(y), \quad (5)$$

where  $\delta S$  represents the area on the spherical surface and  $\delta P$  represents the area on the projection plane,  $x \in (-\pi, \pi)$ ,  $y \in (-\frac{\pi}{2}, \frac{\pi}{2})$ .

From equation 5, we conclude that the ERP distortion is only determined by its degree of latitude. ERP distortion is the heaviest in the polar areas. ERP images suffer a distortion caused by a non-consistency area stretching ratio from an ideal spherical surface. Referred from equation 5, for a input  $X \in \mathbb{R}^{C \times M \times N}$ , the distortion condition map  $C_d \in \mathbb{R}^{1 \times M \times N}$  is derived by:

$$C_d = \cos\left(\frac{m + 0.5 - M/2}{M}\pi\right), \quad (6)$$

where  $m$  is the current height input frames.

Spatial distortion within image frames and the estimation of temporal motion patterns represent significant challenges in Omnidirectional Video Interpolation. In terms of spatial distortion, the distortion within image frames primarily arises from the projection methods used to capture omnidirectional scenes, such as Equirectangular Projection (ERP). Due to the unique characteristics of ERP, such as latitude-dependent deformation, image frames exhibit varying degrees of distortion across different regions. Particularly, objects near the image borders or poles are more susceptible to distortion compared to those in the central regions. This distortion manifests itself as the stretching or compression of objects, leading to inconsistencies in object size and shape throughout the video sequence. Consequently, accurately estimating motion and generating intermediate frames that maintain visual coherence become formidable tasks that require innovative solutions to mitigate the effects of distortion and ensure the fidelity of interpolated frames. Regarding temporal aspects, accurate estimation of temporal motion patterns is also a significant challenge in Omnidirectional Video Interpolation. This includes accurately estimating parameters such as object trajectories, velocities, and accelerations over time within the video sequence. Furthermore, the distortion present in ERP images arises



mainly from latitude-dependent deformation, which manifests itself as distortion in the vertical dimension of the image. It’s noteworthy that objects transitioning from regions near the image center (low latitude) to the upper and lower poles (high latitude) undergo alterations in appearance, including variations in area or volume. This deformation phenomenon, known as depth distortion or spherical distortion, is attributed to the distinct representation of spherical images in ERP projection compared to flat images.

## 4.2 Distortion Priors Using Approaches

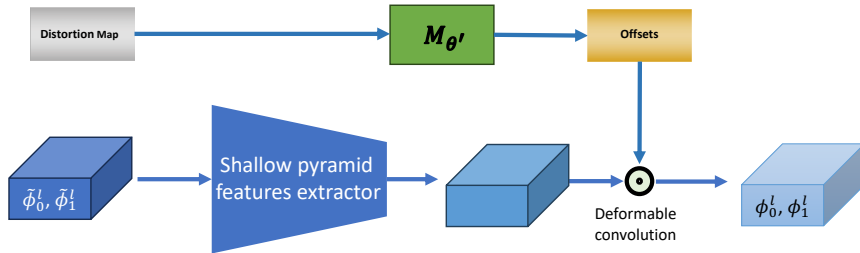


Figure 6: DistortionGuard (A Distortion-aware Features Extractor): The inputs are ERP frames or features  $\tilde{\phi}_0^l$  and  $\tilde{\phi}_1^l$  that are extracted from the last-level encoder. Then the extractor outputs less distorted features  $\phi_0^l$  and  $\phi_1^l$ .

### 4.2.1 DistortionGuard: A Distortion-Aware Pyramid Feature Extractor

Previous methods tend to treat  $C_d$  as an additional input of  $X$  (Nishiyama et al., 2021), or re-weighting parameters by  $C_d$  (Khasanova & Frossard, 2019). However, continuous and amorphous distortions cannot be adequately fitted by scattering and structured convolution operations. Therefore, we intend to design a novel block to continuously learn distorted patterns. In video frame interpolation tasks, the deformable mechanism is proposed to align features between adjacent frames (Tian et al., 2020; Wang et al., 2020b). Unlike standard DCN (Dai et al., 2017), which calculates offsets from the input feature map, offsets are calculated from bi-directional optical flow in VSR pipelines.

Drawing inspiration from feature-level flow warping techniques in Video Super-Resolution (VSR), Yu et al. (2023) employs feature-level warping operations to modulate Equirectangular Projection (ERP) distortion. To learn distortions and extract features meanwhile, we propose the block DistortionGuard to modulate ERP distortion, as shown in  $C_d$  is utilized to calculate the deformable offsets. More specifically, we apply a standard deformable convolution layer with a substituted input for offset calculation. Modulated less distorted features  $\tilde{\phi}_0^l$  and  $\tilde{\phi}_1^l$  are extracted as:

$$\tilde{\phi}_0^l, \tilde{\phi}_1^l = H_{\text{DCN}}(\tilde{\phi}_0, \tilde{\phi}_1, H_{\text{offset}}(C_d)), \quad (7)$$

where  $H_{\text{DCN}(\cdot)}$  denotes standard deformable convolution layer (Zhu et al., 2019). DistortionGuard is designed to address the challenges posed by ERP distortion by incorporating prior knowledge of distortion patterns into feature extraction. By employing deformable convolution layers, DistortionGuard effectively modulates ERP distortion to enhance feature extraction.

### 4.2.2 OmniFTB: Omnidirectional Distortion Feature Transform Block

Unlike DistortionGuard, which uses priors in the feature extraction stage, the affine transformation is an efficient way to perform feature-wise transformations (Dumoulin et al., 2018). Consequently, in the intermediate feature reconstruction of our method, we propose another block considering ERP priors.

For the feature output from the extraction stage, the distortion is modulated successfully. So we devise a distortion-aware feature transform block (OmniFTB) to apply an affine transformation with a pair of distortion-based parameters. In OmniFTB, a mapping function  $M_{\theta'}$ , based on ERP distortion condition map

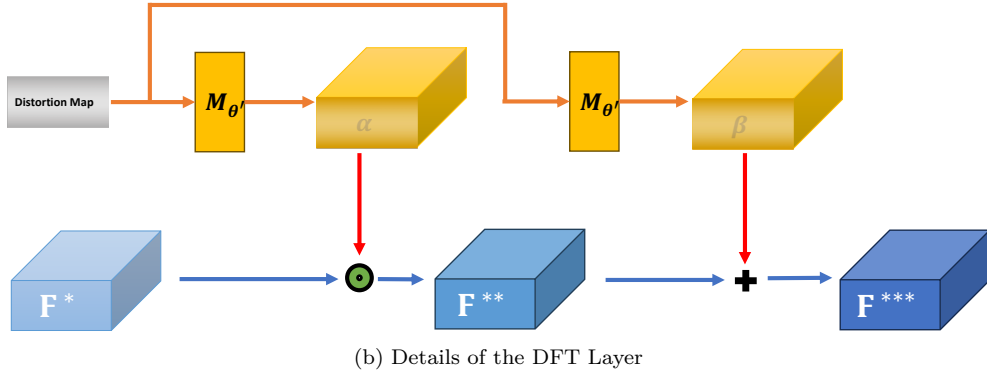
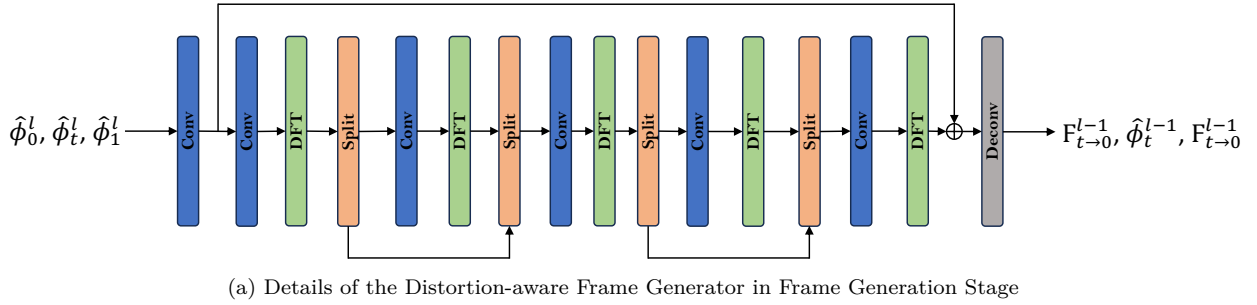


Figure 7: OmniFTB (A Distortion-aware Frame Generator): (a) shows the details of OmniFTB that is composed of Distortion-aware Feature Transform (DFT) layers and other parts; (b) shows the details of a DFT layer using affine transformation. It transforms the feature  $F^*$  from the last convolution layer with the parameter from the ERP distortion map into the feature with distortion  $F^{***}$ . Hence DFT layers recover ERP distortion from less distorted features.

$C_d$  is learned at first,

$$M_{\theta'} : C_d \mapsto (\alpha, \beta), \quad (8)$$

where  $(\alpha, \beta)$  is the parameters to apply affine transformation. After obtaining  $(\alpha, \beta)$  from conditions, the transformation is carried out by scaling and shifting feature maps in the proposed DFT block:

$$F^{***} = DFT(F^* | \alpha, \beta) = \alpha \odot F^* + \beta, \quad (9)$$

where  $F^{***}$  denotes the intermediate feature maps, whose dimension is the same as  $\alpha$  and  $\beta$ , and  $\odot$  is referred to element-wise multiplication, i.e., Hadamard product. Since the spatial dimensions are preserved, the SFT layer not only performs feature-wise manipulation but also spatial-wise transformation. Figure 7. (b) shows an example of implementing DFT block embedded in the intermediate frame generating decoder. The mapping function  $M_{\theta'}$  can be arbitrary functions. In this study, we use a neural network for  $M_{\theta'}$  so that it can be optimized end-to-end with the Omni-VFI branch. OmniFTB complements DistortionGuard by focusing on intermediate feature reconstruction. By applying an affine transformation with distortion-based parameters, OmniFTB effectively leverages ERP distortion priors to transform feature maps for accurate intermediate frame generation.

## 5 Experiments

### 5.1 Implementation Details

We have implemented the proposed algorithm in PyTorch and utilized the 360VFI dataset to train 360VFI Net from scratch. Our model is optimized by AdamW (Loshchilov & Hutter, 2019) algorithm for 300 epochs

with a total batch size of 8 on Two NVIDIA Tesla V100 GPUs. Initially, the learning rate is set to  $1 \times 10^{-4}$  and gradually decays to  $1 \times 10^{-5}$  following a cosine attenuation schedule. Throughout the training process, we refrained from applying augmentation techniques such as rotating and random cropping to triplet samples. This decision was made due to the rigid nature of latitude-dependent distortion.

## 5.2 Evaluation and Comparison

We conducted comparative experiments to evaluate the performance of 360VFI Net against existing methods. We utilized the first omnidirectional video dataset 360VFI we proposed and compared our method with several common VFI approaches. We use the WSS-L1 Loss (Baniya et al., 2023) as the loss function to train 360VFI Net. Smooth L1 loss acts as both L1 and L2 losses conditioned to a hyper-parameter  $\beta$ . It combines the advantages of L1-loss (steady gradients for large values) and L2-loss (less oscillation during update when values are small). Thus, it is less sensitive to outliers and prevents exploding gradients in some cases. However, the loss functions used for conventional images and videos do not take into account the unique nature of ERP frames. Distortion across latitude present in ERP frames can cause learning-based models to be easily influenced by high errors in prediction across polar regions. Therefore, following in the footsteps of WS-PSNR, a Weighted Spherically Smooth-L1 (WSS-L1) Loss function was proposed in Baniya et al. (2023) for taking distortion into consideration along with Smooth-L1 loss,

$$\mathbf{WSS-L1Loss} = \begin{cases} \left(\frac{0.5(GT-HR)^2}{\beta}\right) \times \psi, & \text{if } |GT - HR| < \beta \\ (|GT - HR| - 0.5\beta) \times \psi, & \text{otherwise} \end{cases} \quad (10)$$

where  $\psi$  is the ERP distortion map and  $\beta$  is a hyper-parameter.

We compared the proposed 360VFI Net module with the following methods: IFRNet, DQBC, EMA-VFI, EBME and UPR-Net. We employed the following evaluation metrics to assess the performance of different interpolation methods: Peak Signal-to-Noise Ratio (PSNR), Structural Similarity Index (SSIM), Weighted PSNR (WS-PSNR) (Sun et al., 2017b) and Weighted Structural Similarity Index (WS-SSIM) (Zhou et al., 2018). WS-PSNR extends PSNR by considering the importance of different regions in ODV, calculating PSNR values with weighting factors to emphasize regions of interest, such as central regions with high visual significance. Similarly, WS-SSIM extends SSIM by incorporating weighted factors to account for the perceptual importance of different regions in ODV. It provides a more accurate assessment of perceptual quality considering distortion. With the comprehensive evaluation metrics, we aim to thoroughly evaluate the performance of Omni-VFI methods on four settings of different motion extents, considering both fidelity to ground truth and perceptual quality across the entire omnidirectional view.

Table 3: Quantitative comparison of Omni-VFI results on the dataset 360VFI

Method	Easy		Middle			Hard			Extreme			
	PSNR↑	SSIM↑	WS-PSNR↑	WS-SSIM↑	PSNR↑	SSIM↑	WS-PSNR↑	WS-SSIM↑	PSNR↑	SSIM↑	WS-PSNR↑	WS-SSIM↑
IFRNet Kong et al. (2022)	34.38/0.9685	33.90/0.9538	28.03/0.9136	28.89/0.9047	26.91/0.8905	27.74/0.8724	24.43/0.8421	24.80/0.7999				
DQBC Zhou et al. (2023)	34.06/0.9622	33.51/0.9449	26.33/0.8891	27.35/0.8776	25.14/0.8567	26.02/0.8329	22.81/0.7967	23.26/0.7410				
EMA-VFI Zhang et al. (2023)	33.92/0.9681	33.40/0.9529	27.45/0.9112	28.37/0.9024	26.88/0.8985	27.64/0.8817	24.26/0.8493	24.89/0.8161				
EBME Jin et al. (2023b)	33.93/0.9613	33.48/0.9447	26.27/0.8884	27.35/0.8772	25.08/0.8561	25.97/0.8318	22.84/0.7975	23.23/0.7403				
UPR-Net Jin et al. (2023a)	34.03/0.9686	33.45/0.9535	27.47/0.9116	28.42/0.9024	26.89/0.8988	27.72/0.8816	24.34/0.8507	24.85/0.8157				
Ours	<b>34.48/0.9687</b>	<b>33.95/0.9537</b>	<b>28.13/0.9154</b>	<b>28.96/0.9060</b>	<b>27.41/0.9028</b>	<b>27.81/0.8879</b>	<b>25.52/0.9021</b>	<b>25.63/0.8517</b>				

### 5.2.1 Quantitative comparison

The evaluation results, summarized in Table 3, demonstrate the effectiveness of our 360VFI Net compared to competing methods. Our method consistently achieves superior performance across all metrics evaluated, especially in hard and extreme settings, showcasing its ability to generate high-quality omnidirectional frames in large vertical motion. Specifically, the higher PSNR and SSIM scores indicate better reconstruction fidelity and perceptual quality of the interpolated frames. Moreover, the incorporation of weighted metrics, WS-PSNR and WS-SSIM, further highlights the robustness of our method in handling distortions and variations in ODV sequences.



Figure 8: Qualitative comparisons visualization of five previous SOTA VFI approaches

### 5.2.2 Qualitative comparison

In addition to quantitative evaluation, we conducted a qualitative comparison to visually assess the performance of our proposed 360VFI Net compared to other state-of-the-art methods in plane VFI. We present a figure below illustrating the generated intermediate frames by different methods alongside the ground truth intermediate frames. As depicted in Figure 8, our 360VFI Net consistently produces visually pleasing and high-quality intermediate frames that closely resemble the ground truth frames. The results interpolation exhibits smooth transitions and preserves details effectively, demonstrating the robustness and efficacy of our method in handling Omni-VFI tasks. In contrast, the results from other methods may suffer from artifacts or distortion, leading to less faithful representations of the ground truth frames.

Table 4: Ablation Study on Proposed Block

DistortionGuard	OmniFTB	Easy				Middle				Hard			Extreme		
		PSNR $\uparrow$	SSIM $\uparrow$	WS-PSNR $\uparrow$	WS-SSIM $\uparrow$	PSNR $\uparrow$	SSIM $\uparrow$	WS-PSNR $\uparrow$	WS-SSIM $\uparrow$	PSNR $\uparrow$	SSIM $\uparrow$	WS-PSNR $\uparrow$	SSIM $\uparrow$	WS-PSNR $\uparrow$	SSIM $\uparrow$
×	×	33.65/0.9413	33.32/0.9401	27.51/0.9006	27.55/0.8997	26.57/0.8963	26.76/0.8792	24.63/0.8947	24.69/0.8401						
✓	×	34.05/0.9565	33.66/0.9487	27.79/0.9087	28.24/0.9036	27.19/0.8990	27.27/0.8830	25.00/0.8975	25.14/0.8529						
×	✓	33.97/0.9659	33.64/0.9480	27.73/0.9072	28.14/0.9022	27.05/0.8965	27.29/0.8836	25.02/0.8981	25.09/0.8522						
✓	✓	<b>34.48/0.9687</b>	<b>33.95/0.9537</b>	<b>28.13/0.9154</b>	<b>28.96/0.9060</b>	<b>27.41/0.9028</b>	<b>27.81/0.8879</b>	<b>25.52/0.9021</b>	<b>25.63/0.8617</b>						

### 5.3 Ablation Study

To validate the effectiveness of the two key modules, DistortionGuard and OmniFTB, within 360VFI Net, we conducted ablation experiments. In these experiments, we systematically removed each module and evaluated its impact on the final performance. Specifically, in the DistortionGuard module ablation experiment, we constructed a variant of 360VFI Net without the DistortionGuard module and compared it to the complete 360VFI Net. Similarly, in the OmniFTB module ablation experiment, we designed a variant of 360VFI Net without the OmniFTB module and contrasted it with the version containing the complete architecture. We maintained the same dataset and training settings and compared the performance of the two versions. Table 4 shows that both ablated versions exhibited a noticeable drop in performance compared to the complete 360VFI Net, highlighting the importance of both DistortionGuard and OmniFTB in achieving optimal results.

The results of the ablation experiments demonstrate the significant impact of the DistortionGuard and OmniFTB modules on the performance of 360VFI Net. Their presence enhances the model’s robustness and accuracy, providing crucial support for Omnidirectional Video Frame Interpolation tasks. These findings further substantiate the effectiveness and reliability of 360VFI Net in handling omnidirectional videos, laying a solid foundation for future research and applications.

---

## 6 Conclusion

In this paper, we have devised a dataset and benchmark termed 360VFI for Omnidirectional Video Frame Interpolation. We provide the first dataset for Omnidirectional Video Frame Interpolation, which is collected and cleaned from multiple sources and tailored into a triplet format. 360VFI dataset has four evaluation settings, serving as a benchmark for various extents of motion in Omnidirectional Videos and facilitating future research in this field. Furthermore, the proposed 360VFI Net uniquely incorporates ERP distortion priors in both the feature extraction stage and the frame generation stage, employing different customized methods for each stage. It first extracts less distorted features of two input frames according to the distortion map and then gradually generates the target ERP frame using parameterized affine transformation to recover the distortion. We anticipate that our contributions will inspire further advancements in omnidirectional video processing techniques, ultimately enhancing the immersive viewing experience.

## References

- Arbind Agrahari Baniya, Tsz-Kwan Lee, Peter W. Eklund, and Sunil Aryal. Omnidirectional video super-resolution using deep learning. *IEEE Transactions on Multimedia*, pp. 1–15, 2023. doi: 10.1109/TMM.2023.3267294.
- Wenbo Bao, Wei-Sheng Lai, Xiaoyun Zhang, Zhiyong Gao, and Ming-Hsuan Yang. Memc-net: Motion estimation and motion compensation driven neural network for video interpolation and enhancement. *IEEE Transactions on Pattern Analysis and Machine Intelligence*, 2018. doi: 10.1109/TPAMI.2019.2941941.
- Wenbo Bao, Wei-Sheng Lai, Chao Ma, Xiaoyun Zhang, Zhiyong Gao, and Ming-Hsuan Yang. Depth-aware video frame interpolation. In *Proceedings of the IEEE/CVF conference on computer vision and pattern recognition*, pp. 3703–3712, 2019.
- Keshav Bhandari, Bin Duan, Gaowen Liu, Hugo Latapie, Ziliang Zong, and Yan Yan. Learning omnidirectional flow in 360 video via siamese representation. In *European Conference on Computer Vision*, pp. 557–574. Springer, 2022.
- Xianhang Cheng and Zhenzhong Chen. Multiple video frame interpolation via enhanced deformable separable convolution. *IEEE Transactions on Pattern Analysis and Machine Intelligence*, 44(10):7029–7045, 2021.
- Myungsub Choi, Heewon Kim, Bohyung Han, Ning Xu, and Kyoung Mu Lee. Channel attention is all you need for video frame interpolation. In *AAAI*, 2020.
- Taco S Cohen, Mario Geiger, Jonas Köhler, and Max Welling. Spherical cnns. *arXiv preprint arXiv:1801.10130*, 2018.
- Benjamin Coors, Alexandru Paul Condurache, and Andreas Geiger. Spherenet: Learning spherical representations for detection and classification in omnidirectional images. In *Proceedings of the European Conference on Computer Vision (ECCV)*, September 2018.
- Jifeng Dai, Haozhi Qi, Yuwen Xiong, Yi Li, Guodong Zhang, Han Hu, and Yichen Wei. Deformable convolutional networks. In *Proceedings of the IEEE international conference on computer vision*, pp. 764–773, 2017.
- Alexey Dosovitskiy, Philipp Fischer, Eddy Ilg, Philip Häusser, Caner Hazirbas, Vladimir Golkov, Patrick van der Smagt, Daniel Cremers, and Thomas Brox. FlowNet: Learning optical flow with convolutional networks. In *2015 IEEE International Conference on Computer Vision (ICCV)*, 2015.
- Vincent Dumoulin, Ethan Perez, Nathan Schucher, Florian Strub, Harm de Vries, Aaron Courville, and Yoshua Bengio. Feature-wise transformations. *Distill*, 2018. doi: 10.23915/distill.00011. <https://distill.pub/2018/feature-wise-transformations>.
- Carlos Esteves, Christine Allen-Blanchette, Ameesh Makadia, and Kostas Daniilidis. Learning so (3) equivariant representations with spherical cnns. In *Proceedings of the European Conference on Computer Vision (ECCV)*, pp. 52–68, 2018.

- 
- Hou-Ning Hu, Yen-Chen Lin, Ming-Yu Liu, Hsien-Tzu Cheng, Yung-Ju Chang, and Min Sun. Deep 360 pilot: Learning a deep agent for piloting through 360 sports videos. In *2017 IEEE Conference on Computer Vision and Pattern Recognition (CVPR)*, pp. 1396–1405. IEEE, 2017.
- Zhewei Huang, Tianyuan Zhang, Wen Heng, Boxin Shi, and Shuchang Zhou. Real-time intermediate flow estimation for video frame interpolation. In *Proceedings of the European Conference on Computer Vision (ECCV)*, 2022.
- Huaizu Jiang, Deqing Sun, Varan Jampani, Ming-Hsuan Yang, Erik Learned-Miller, and Jan Kautz. Super slomo: High quality estimation of multiple intermediate frames for video interpolation. In *2018 IEEE/CVF Conference on Computer Vision and Pattern Recognition*, 2018a.
- Huaizu Jiang, Deqing Sun, Varun Jampani, Ming-Hsuan Yang, Erik Learned-Miller, and Jan Kautz. Super slomo: High quality estimation of multiple intermediate frames for video interpolation. In *Proceedings of the IEEE conference on computer vision and pattern recognition*, pp. 9000–9008, 2018b.
- Xin Jin, Longhai Wu, Jie Chen, Youxin Chen, Jayoon Koo, and Cheul-hee Hahm. A unified pyramid recurrent network for video frame interpolation. In *Proceedings of the IEEE conference on computer vision and pattern recognition*, 2023a.
- Xin Jin, Longhai Wu, Guotao Shen, Youxin Chen, Jie Chen, Jayoon Koo, and Cheul-hee Hahm. Enhanced bi-directional motion estimation for video frame interpolation. In *Proceedings of the IEEE/CVF Winter Conference on Applications of Computer Vision (WACV)*, 2023b.
- Kyoungkook Kang and Sunghyun Cho. Interactive and automatic navigation for 360° video playback. *ACM Trans. Graph.*, 38(4), jul 2019.
- Reanta Khasanova and Pascal Frossard. Geometry aware convolutional filters for omnidirectional images representation. In *International Conference on Machine Learning*, 2019.
- Lingtong Kong, Chunhua Shen, and Jie Yang. Fastflownet: A lightweight network for fast optical flow estimation. In *2021 IEEE International Conference on Robotics and Automation (ICRA)*, 2021.
- Lingtong Kong, Boyuan Jiang, Donghao Luo, Wenqing Chu, Xiaoming Huang, Ying Tai, Chengjie Wang, and Jie Yang. Ifrnet: Intermediate feature refine network for efficient frame interpolation. In *Proceedings of the IEEE/CVF Conference on Computer Vision and Pattern Recognition (CVPR)*, 2022.
- Johannes Kopf. 360 video stabilization. *ACM Transactions on Graphics (TOG)*, 35(6):1–9, 2016.
- Hyeongmin Lee, Taeoh Kim, Tae-young Chung, Daehyun Pak, Yuseok Ban, and Sangyoum Lee. Adacof: Adaptive collaboration of flows for video frame interpolation. In *Proceedings of the IEEE/CVF conference on computer vision and pattern recognition*, pp. 5316–5325, 2020.
- Chen Li, Mai Xu, Lai Jiang, Shanyi Zhang, and Xiaoming Tao. Viewport proposal cnn for 360° video quality assessment. In *2019 IEEE/CVF Conference on Computer Vision and Pattern Recognition (CVPR)*, pp. 10169–10178. IEEE, 2019a.
- Jia Li, Jinming Su, Changqun Xia, and Yonghong Tian. Distortion-adaptive salient object detection in 360° omnidirectional images. *IEEE Journal of Selected Topics in Signal Processing*, 14(1):38–48, 2019b.
- Yiheng Li, Connelly Barnes, Kun Huang, and Fang-Lue Zhang. Deep 360 optical flow estimation based on multi-projection fusion. In *European Conference on Computer Vision*, pp. 336–352. Springer, 2022.
- Gucan Long, Laurent Kneip, Jose M Alvarez, Hongdong Li, Xiaohu Zhang, and Qifeng Yu. Learning image matching by simply watching video. In *Computer Vision—ECCV 2016: 14th European Conference, Amsterdam, The Netherlands, October 11–14, 2016, Proceedings, Part VI 14*, pp. 434–450. Springer, 2016.
- I. Loshchilov and F. Hutter. Decoupled weight decay regularization. In *7th International Conference on Learning Representations*, 2019.

- 
- Simone Meyer, Oliver Wang, Henning Zimmer, Max Grosse, and Alexander Sorkine-Hornung. Phase-based frame interpolation for video. In *2015 IEEE Conference on Computer Vision and Pattern Recognition (CVPR)*, pp. 1410–1418, 2015. doi: 10.1109/CVPR.2015.7298747.
- Simone Meyer, Abdelaziz Djelouah, Brian McWilliams, Alexander Sorkine-Hornung, Markus Gross, and Christopher Schroers. Phasenet for video frame interpolation. In *Proceedings of the IEEE Conference on Computer Vision and Pattern Recognition*, pp. 498–507, 2018.
- Mark Roman Miller, Fernanda Herrera, Hanseul Jun, James A Landay, and Jeremy N Bailenson. Personal identifiability of user tracking data during observation of 360-degree vr video. *Scientific Reports*, 10(1): 17404, 2020.
- Rafael Monroy, Sebastian Lutz, Tejo Chalasani, and Aljosa Smolic. Salnet360: Saliency maps for omnidirectional images with cnn. *Signal Processing: Image Communication*, 69:26–34, 2018.
- Cuong Nguyen, Stephen DiVerdi, Aaron Hertzmann, and Feng Liu. Vremiere: In-headset virtual reality video editing. In *Proceedings of the 2017 CHI Conference on Human Factors in Computing Systems*, pp. 5428–5438, 2017.
- Simon Niklaus and Feng Liu. Softmax splatting for video frame interpolation. In *Proceedings of the IEEE/CVF Conference on Computer Vision and Pattern Recognition (CVPR)*, 2020.
- Simon Niklaus, Long Mai, and Feng Liu. Video frame interpolation via adaptive convolution. In *Proceedings of the IEEE Conference on Computer Vision and Pattern Recognition*, pp. 670–679, 2017.
- Akito Nishiyama, Satoshi Ikehata, and Kiyoharu Aizawa. 360° single image super resolution via distortion-aware network and distorted perspective images. In *2021 IEEE International Conference on Image Processing (ICIP)*, pp. 1829–1833, 2021. doi: 10.1109/ICIP42928.2021.9506233.
- Junheum Park, Chul Lee, and Chang-Su Kim. Asymmetric bilateral motion estimation for video frame interpolation. In *Proceedings of the IEEE/CVF International Conference on Computer Vision (ICCV)*, 2021.
- Khurram Soomro, Amir Roshan Zamir, and Mubarak Shah. Ucf101: A dataset of 101 human actions classes from videos in the wild. *CoRR*, 2012.
- Yu-Chuan Su and Kristen Grauman. Kernel transformer networks for compact spherical convolution. In *Proceedings of the IEEE/CVF Conference on Computer Vision and Pattern Recognition*, pp. 9442–9451, 2019.
- Deqing Sun, Xiaodong Yang, Ming-Yu Liu, and Jan Kautz. Pwc-net: Cnns for optical flow using pyramid, warping, and cost volume. In *2018 IEEE/CVF Conference on Computer Vision and Pattern Recognition*, 2018.
- Yule Sun, Ang Lu, and Lu Yu. Weighted-to-spherically-uniform quality evaluation for omnidirectional video. *IEEE Signal Processing Letters*, 24(9):1408–1412, 2017a. doi: 10.1109/LSP.2017.2720693.
- Yule Sun, Ang Lu, and Lu Yu. Weighted-to-spherically-uniform quality evaluation for omnidirectional video. *IEEE signal processing letters*, 24(9):1408–1412, 2017b.
- Chengzhou Tang, Oliver Wang, Feng Liu, and Ping Tan. Joint stabilization and direction of 360° videos. *ACM Transactions on Graphics (TOG)*, 38(2):1–13, 2019.
- Zachary Teed and Jia Deng. Raft: Recurrent all-pairs field transforms for optical flow. In *Computer Vision – ECCV 2020*, 2020.
- Yapeng Tian, Yulun Zhang, Yun Fu, and Chenliang Xu. Tdan: Temporally-deformable alignment network for video super-resolution. In *The IEEE Conference on Computer Vision and Pattern Recognition (CVPR)*, June 2020.

- 
- Antonio Torralba. Recognizing scene viewpoint using panoramic place representation. In *Proceedings of the 2012 IEEE Conference on Computer Vision and Pattern Recognition (CVPR)*, CVPR '12, pp. 2695–2702, USA, 2012. IEEE Computer Society. ISBN 9781467312264.
- Longguang Wang, Yulan Guo, Yingqian Wang, Juncheng Li, Shuhang Gu, Radu Timofte, Ming Cheng, Haoyu Ma, Qiufang Ma, Xiaopeng Sun, et al. Ntire 2023 challenge on stereo image super-resolution: Methods and results. In *Proceedings of the IEEE/CVF Conference on Computer Vision and Pattern Recognition*, pp. 1346–1372, 2023.
- Ning-Hsu Wang, Bolivar Solarte, Yi-Hsuan Tsai, Wei-Chen Chiu, and Min Sun. 360sd-net: 360 stereo depth estimation with learnable cost volume. In *2020 IEEE International Conference on Robotics and Automation (ICRA)*, pp. 582–588. IEEE, 2020a.
- Xintao Wang, Ke Yu, Chao Dong, and Chen Change Loy. Recovering realistic texture in image super-resolution by deep spatial feature transform. In *The IEEE Conference on Computer Vision and Pattern Recognition (CVPR)*, June 2018.
- Xintao Wang, Ke Yu, Kelvin C.K. Chan, Chao Dong, and Chen Change Loy. Basicsr. <https://github.com/xinntao/BasicSR>, 2020b.
- Junjie Wu, Changqun Xia, Tianshu Yu, and Jia Li. View-aware salient object detection for 360  $\{\backslash\deg\}$  omnidirectional image. *arXiv preprint arXiv:2209.13222*, 2022.
- Xiangyu Xu, Li Siyao, Wenxiu Sun, Qian Yin, and Ming-Hsuan Yang. Quadratic video interpolation. In *Advances in Neural Information Processing Systems*, 2019.
- Tianfan Xue, Baian Chen, Jiajun Wu, Donglai Wei, and William T Freeman. Video enhancement with task-oriented flow. *International Journal of Computer Vision (IJCV)*, 127(8):1106–1125, 2019.
- Jiachen Yang, Tianlin Liu, Bin Jiang, Wen Lu, and Qinggang Meng. Panoramic video quality assessment based on non-local spherical cnn. *IEEE Transactions on Multimedia*, 23:797–809, 2021. doi: 10.1109/TMM.2020.2990075.
- Fanghua Yu, Xintao Wang, Mingdeng Cao, Gen Li, Ying Shan, and Chao Dong. Osrt: Omnidirectional image super-resolution with distortion-aware transformer. In *Proceedings of the IEEE/CVF Conference on Computer Vision and Pattern Recognition*, pp. 13283–13292, 2023.
- Guozhen Zhang, Yuhan Zhu, Haonan Wang, Youxin Chen, Gangshan Wu, and Limin Wang. Extracting motion and appearance via inter-frame attention for efficient video frame interpolation. In *Proceedings of the IEEE/CVF Conference on Computer Vision and Pattern Recognition*, pp. 5682–5692, 2023.
- Yun Zhang, Fang-Lue Zhang, Yu-Kun Lai, and Zhe Zhu. Efficient propagation of sparse edits on 360 panoramas. *Computers and Graphics*, 96:61–70, 2021.
- Ziheng Zhang, Yanyu Xu, Jingyi Yu, and Shenghua Gao. Saliency detection in 360 videos. In *Proceedings of the European conference on computer vision (ECCV)*, pp. 488–503, 2018.
- Yinjie Zhao, Lichen Zhao, Qian Yu, Lu Sheng, Jing Zhang, and Dong Xu. Distortion-aware transformer in 360° salient object detection. In *Proceedings of the 31st ACM International Conference on Multimedia*, MM '23, pp. 499–508, New York, NY, USA, 2023. Association for Computing Machinery. ISBN 9798400701085. doi: 10.1145/3581783.3612025. URL <https://doi.org/10.1145/3581783.3612025>.
- Chang Zhou, Jie Liu, Jie Tang, and Gangshan Wu. Video frame interpolation with densely queried bilateral correlation. In Edith Elkind (ed.), *Proceedings of the Thirty-Second International Joint Conference on Artificial Intelligence, IJCAI-23*, pp. 1786–1794. International Joint Conferences on Artificial Intelligence Organization, 8 2023. doi: 10.24963/ijcai.2023/198. URL <https://doi.org/10.24963/ijcai.2023/198>. Main Track.



---

Yufeng Zhou, Mei Yu, Hualin Ma, Hua Shao, and Gangyi Jiang. Weighted-to-spherically-uniform ssim objective quality evaluation for panoramic video. In *2018 14th IEEE International Conference on Signal Processing (ICSP)*, pp. 54–57. IEEE, 2018.

Xizhou Zhu, Han Hu, Stephen Lin, and Jifeng Dai. Deformable convnets v2: More deformable, better results. In *Proceedings of the IEEE/CVF conference on computer vision and pattern recognition*, pp. 9308–9316, 2019.

## **A Appendix**

You may include other additional sections here.